Switching Mechanism in Ferromagnetic Nanorings

Wen Zhang* and Stephan Haas†

Department of Physics and Astronomy,

University of Southern California,

Los Angeles, CA 90089, USA

Abstract

Ferromagnetic rings exhibit many novel physical phenomena with promise for potential applications. Here, we focus on switching processes which are fundamental properties of magnetic systems and are especially crucial for data storage applications. A brief introduction on the advantages of ring geometries is presented, followed by a background survey of the model and methods to study nanomagnetic elements. The relevant magnetic states identified until now are discussed, with special emphasis given to vortex, onion, and twisted states. Such states are potential candidates for data storage applications. Switching processes under uniform fields are categorized into three types, and their mechanisms are explained in detail. In particular, explanations from a topological point of view are shown to be enlightening. We conclude with a brief discursion of circular field switching and data storage applications of magnetic nanorings.

Keywords: ring, magnet, switching, hysteresis

*Electronic address: zhangwen@usc.edu

†Electronic address: shaas@usc.edu

Contents

I. INTRODUCTION

During the last two decades, tremendous effort has been devoted to micron and submicron magnetic elements, motivated both by fundamental scientific interest, such as novel magnetic states and switching processes [1, 2, 3], and by their potential for technological applications, such as magnetic random access memory (MRAM) [4, 5] and magnetic sensors [6, 7]. Characterizing the magnetic properties of nanostructures is a challenging task, as their shape significantly influences their physical response. Significant work has been invested into identifying the geometries which offer the simplest, fastest, and most reproducible switching mechanisms. Particular attention has focused on magnetic structures with high-symmetry geometries, such as circular disks and squares, since spin configurations with high symmetry are expected for these elements, which in turn are believed to yield simple and reproducible memory states.

In analogy to the traditional approach to encode information in dipolar-like giant spins, quasi-uniform single domain states have been proposed and intensively studied. However, these typically suffer from three fundamental disadvantages: (i) they are sensitive to edge roughness so that the switching field typically has a broad distribution; (ii) because of the long-ranged dipolar interactions between separate elements, high density arrays are hard to achieve; (iii) they cannot be made to be too small due to the superparamagnetism effect. To overcome these problems, use of the magnetic vortex state in disc geometries (see Fig. 1(a)) has been suggested, since it is insensitive to edge imperfections and entirely avoids the superparamagnetism effect. Moreover, the zero in-plane stray field opens the possibility of high density storage. Nevertheless, the vortex state is stable only in discs of fairly large sizes (diameter over about 100nm) due to the existence of high energy penalty vortex core regions. What is worse, the switching mechanisms for discs are complex and difficult to control. In seeking a solution, ring geometries (see Fig. 1(b)) have been proposed and studied intensively in the last decade. In addition to all the advantages of vortex states in the disc geometry, magnetic rings are completely stray field free and can be stable with diameters as small as 10nm. Taking 10nm spacing into account, ring arrays give an ultimate area storage density of about $0.25 Tbits/cm^2$ (or $1.6 Tbits/in.^2$), substantially higher than the traditional hard disc area storage density limit. Besides this promising application potential, ring geometries have proven to be a wonderful platform for the investigation of fundamental

physical questions concerning domain walls. [8]

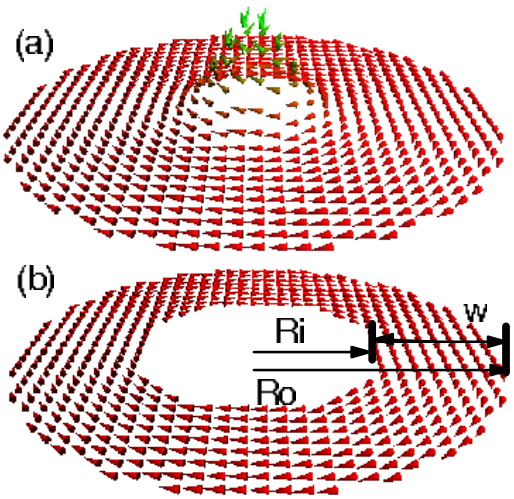

FIG. 1: (color online) Schematic representation of a magnetic vortex state in a disc (a) and a ring (b). The core region where spin points out of plane are exaggerated and represented by the height and green color. R_o and R_i are outer and inner radius of rings and w is their width.

For the study of magnetic properties of structures in micrometer and nanometer dimensions, micromagnetic simulations prove to be a very powerful tool. [9] To study dynamic properties, one has to resort to numerical integration of the Landau-Lifshitz-Gilbert (LLG) equation [10, 11]. For (quasi)static properties, Monte Carlo simulations are also applied extensively. [1] Numerically evaluating the energy of such systems is highly nontrivial because of the long-range character of the dipolar interaction between magnetic moments which contributes to the magnetostatic energy. The complexity of a brute-force calculation is $\mathcal{O}(N^2)$. However, there are several approaches to improve this. The most important two techniques are the Fast Fourier Transform (FFT), which reduces the complexity to $\mathcal{O}(Nlog(N))$, and the Fast Multipole Method (FMM) [12, 13], which reduces the complexity to $\mathcal{O}(N)$ but with fairly large coefficients. Based on these methods, several open software packages are available: OOMMF[14], magpar[15], Nmag[16], ψ-mag [17]. Of these, OOMMF is the most mature and popular one, and has been extensively used worldwide.

This review article is an overview of current research on magnetic rings, with a focus on clarifying their quasistatic properties. We will mainly refer to results in the literature and include some of our own recent findings. Considering the overwhelming amount of literature,

we apologize for the inevitable omission of some important works. The article is organized as follows: in section 2, we cover the basic background needed to study magnetic systems; in section 3, we explain the equilibrium magnetic states (spin configuration) and metastable states in ring geometries; finally, the mechanism of switching processes in rings is discussed in detail in section 4, followed by a brief discussion of data storage applications in section 5.

II. BACKGROUND

In the quasi-classical approximation, the Hamiltonian ($\mathcal{H}$) of a magnetic nanoparticle in a magnetic field consists of four terms: exchange interaction, dipolar interaction, crystalline anisotropy and Zeeman energy. The sum of the first three terms yields the internal energy. If each magnetic moment occupies a site of the underlying crystal lattice, $\mathcal{H}$ is given by

$$\mathcal{H} \;=\; -J \sum_{<i,j>} \vec{S}_i \cdot \vec{S}_j + D \sum_{i,j} \frac{\vec{S}_i \cdot \vec{S}_j - 3(\vec{S}_i \cdot \hat{r}_{ij})(\vec{S}_j \cdot \hat{r}_{ij})}{r_{ij}^3} + U_k - \vec{H} \cdot \sum_i \vec{S}_i, \qquad (1)$$

where $J > 0$ is the ferromagnetic exchange constant (or exchange integral, measured in units of energy), which is assumed to be non-zero only for nearest neighbors, D is the dipolar coupling parameter and $\vec{r}_{ij}$ is the displacement vector between sites i and j. The anisotropy term U_k can take various forms[18], among which the most common are uniaxial anisotropy $U_k = K \sum_i sin^2\theta_i$, where θ_i is the angle $\vec{S}_i$ makes with the easy axis, and cubic anisotropy $U_k = K \sum_i [\alpha_i^2\beta_i^2 + \beta_i^2\gamma_i^2 + \alpha_i^2\gamma_i^2]$, where $\alpha_i, \beta_i, \gamma_i$ are the direction cosines of $\vec{S}_i$. Note that K is the single site anisotropy energy (not an energy density) and that $\vec{S}$ is a dimensionless unit spin vector with magnetic moments $\vec{\mu} = |\mu|\vec{S}$. Experimentally, the materials used are mostly Co, Fe, permalloy and supermalloy. For these materials, the ratio D/Ja^3 falls in the range of 10^{-3} and 10^{-5}, where $a \sim 0.3nm$ is lattice constant. For polycrystalline systems, U_k is usually omitted since the crystalline anisotropy is very small. For epitaxial systems, however, crystalline anisotropy needs to be considered. Generally it stabilizes certain directions and enhances the switching field. It also helps to resist the superparamagnetism effect. The Zeeman term above applies for uniform fields. If this is not the case, the term is adjusted to $\sum_i \vec{S}_i \cdot \vec{H}_i$. The main observables in magnetic systems are the magnetization and susceptibility.

The competition between the various energy terms in $\mathcal{H}$ results in the interesting com-

plexity of magnetic nanostructures. The exchange interaction tends to align spins in the same direction, whereas the dipolar interaction encourages spins to line up along the boundaries, which is the origin of the shape anisotropy. Thus spins align in-plane in a flat element while they point out-of-plane if the thickness is much larger than the lateral dimension. The former case attracts more attention since it exhibits rich new phenomena and is closely related to applications. Plenty of competing configurations exist, including flower, leaf, onion, buckle, and vortex states.

The study of micron and submicron magnetic elements has two major branches: quasistatic properties and dynamics. Here we will focus on the former, in particular on the switching process, a first order phase transition. To understand the switching process, we first discuss in detail all the possible states in magnetic rings. After that, the magnetization reversal mechanism (the hysteresis) is investigated.

Many magnetic phenomena involve vortices and domain walls. From a topological point of view, these are defects. The topological theory of defects [19, 20, 21] can help us to understand the complex creation and annihilation processes during switching. One of the most important principles is the conservation of topological charge. Topological charge is defined as the winding number ω, i.e. a line integral around the defect center:

$$\omega = \frac{1}{2\pi} \oint \nabla\theta(\vec{r}) \cdot d\vec{r}, \tag{2}$$

where θ is the angle between the local magnetic moment and the positive x axis. There are several elementary topological defects in magnetic systems. As is known, a vortex in the bulk has an integer winding number $\omega = 1$ and an antivortex has $\omega = -1$. Furthermore, Tchernyshyov *et al* [20] identified two edge defects with fractional winding numbers $\omega = \pm 1/2$. These four types of elementary topological defects are shown in Fig.2. All the magnetic intricate textures, including domain walls, are composite objects made of some of the above four elementary defects.[20] These defects have several properties: (i) in analogy to Coulomb interaction, two defects with the same winding number sign repel each other, while they attract each other if they have opposite signs of winding number; (ii) the vortex is repelled by the boundary since it has an image "charge" with the same sign; (iii) edge defects are confined to the edge by an effective confining potential; (iv) direct annihilation of two defects with the same sign is prohibited; (v) edge defects can change sign by introducing

a bulk defect; (vi) in sufficiently narrow rings, $\omega = \pm 1/2$ edge defects are degenerate, i.e. they have the same energy, whereas in thick rings the $\omega = +1/2$ will have substantially higher energy than the $\omega = -1/2$ so that it can decay into a vortex $\omega = 1$ and an edge defect $\omega = -1/2$.

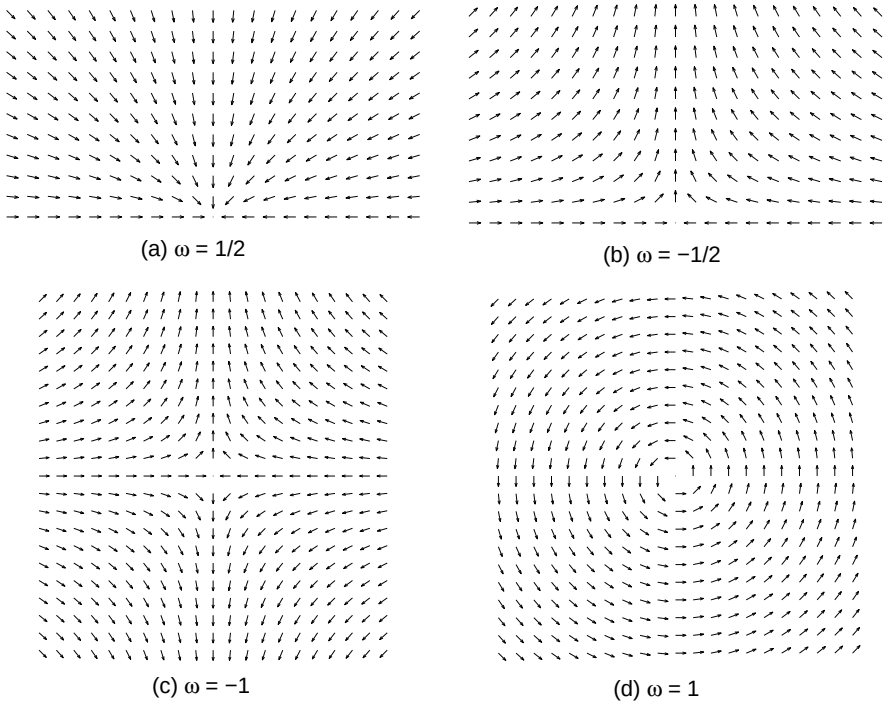

FIG. 2: Elementary topological defects: (a) edge defect ω=1/2, (b) edge defect ω=-1/2, (c) vortex ω=1, (d) antivortex ω=-1.

Concerning experimental fabrication techniques, interested readers can refer to Martin *et al* [2] and Kläui *et al* [22]. Experimentalists are able to produce two kinds of morphology: polycrystalline and epitaxial. In most cases, magnetic rings are made of polycrystalline permalloy, supermalloy and Co, whose crystalline anisotropy is negligible. On the other hand, when one wants to study the effects of anisotropy and underlying lattice structure, epitaxial face centered cubic (fcc), face centered tetragonal (fct) and hexagonal close-packed (hcp) structure Co rings can be produced. The imaging techniques can be classified into two groups: (i) intrusive techniques such as magnetic force microscope (MFM): this method affects the magnetic state of the sample because of the external magnetic field of the tip; (ii) non-intrusive techniques such as Photoemission Electron Microscopes (PEEM) and Scanning Electron Microscopy with Polarization Analysis (SEMPA): the magnetic states remain the

same after the image is scanned. The spatial resolution nowadays can be as high as 10nm. Atomic resolution is also reported by SP-STM [23, 24]. To measure the hysteresis curve, the most popular techniques used are the magneto-optic Kerr effect (MOKE) and SQUID. Other techniques include measurement of the Hall resistance[25] and of the spin-wave spectrum[26]. In most cases, the hysteresis is measured in arrays of nanorings, typically larger than 10×10. Thus the transition field has a range which represents the transition field distribution among these nanoparticles. A few measurements have been reported for single particles where the transition is sharp, but the size of these particles is fairly big.

III. MAGNETIC STATES

A first step in the investigation of the magnetic properties of certain geometries is to identify the competing stable and metastable spin configurations at remanence. This information can be summarized in a geometric phase diagram.

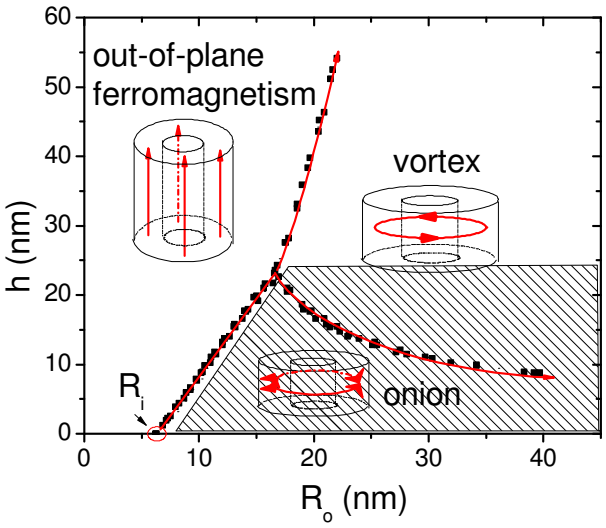

FIG. 3: (color online) Schematic geometric magnetic phase diagram for nanorings with $R_i = 6nm$. Shaded area is the region where the onion state could be (meta)stable, and thus it is of greatest interest.

Several works have been devoted to determining this phase diagram [27, 28, 29] for ring structures. Fig. 3 shows an example with inner radius R_i fixed. Spins point out of plane in parallel when the element height h is much larger than width w. The opposite situation

is of more interest. When $h/w < 2$, there are two possible states: (i) the vortex state (V) (or the flux close state), characterized by the circulation of spins; (ii) the onion state (O) (or the quasi uniform state), characterized by two head-to-head domain walls. The vortex state is the only single domain state in ring structures. Because of the resemblance to strips, magnetic rings hold a lot of multi-domain states, such as onion states and various twisted states discussed in detail below. The onion state has two domains, separated by two head-to-head domain walls. The two domains are sometimes referred to two arms. Since the domain walls in ring geometries are well confined, ring magnets serve as a perfect platform to study the motion of domain walls as well as the interaction between them [8, 22].

All the interesting behavior of magnetic systems stems from the fact that there is a great variety of metastable states. Several states may be stable at remanence depending on the history how remanence is reached. One can see from Fig. 3 that the dominant phase for thin films is the vortex state, but the onion state is actually a metastable state in a very large region. If the remanence state is obtained by relaxing from saturation, it is usually an onion state. A remanent state phase diagram is given for Co nanorings [30] where the onion state area is significantly increased. As mentioned above, onion states are characterized by two head-to-head domain walls[31] which have long been studied in magnetic strips. Two kinds of head-to-head domain walls exist: transverse domain walls in thin rings, see Fig. 4(a) and vortex walls in wide rings, see Fig. 4(b). A geometric phase diagram (see Fig. 5) for the two head-to-head domain walls was found by Laufenberg et al [32].

Note that the phase diagram was obtained by relaxing the system from saturation, so it does not represent the ground state of the system at zero field and shows no vortex state at all. One can see from the Fig. 5(b) that analytical calculations tend to favor vortex walls while simulations tend to favor transverse walls compared with the experimental result. It results from the fact that there is an energy barrier between vortex walls and transverse walls. Analytical calculations give the lower energy state, while real systems can stay in the local minimum with transverse walls. Simulations are performed in zero temperature, so that it is harder to form vortex walls than in the experimental situation, where thermal fluctuation can help the system overcome the barrier.

From a topological point of view, the transverse wall is composed of a $\omega = 1/2$ defect at the outer edge and a $\omega = -1/2$ defect at the inner edge[20]. The vortex wall is composed of two $\omega = -1/2$ defects respectively at the outer and inner edge together with a $\omega = +1$

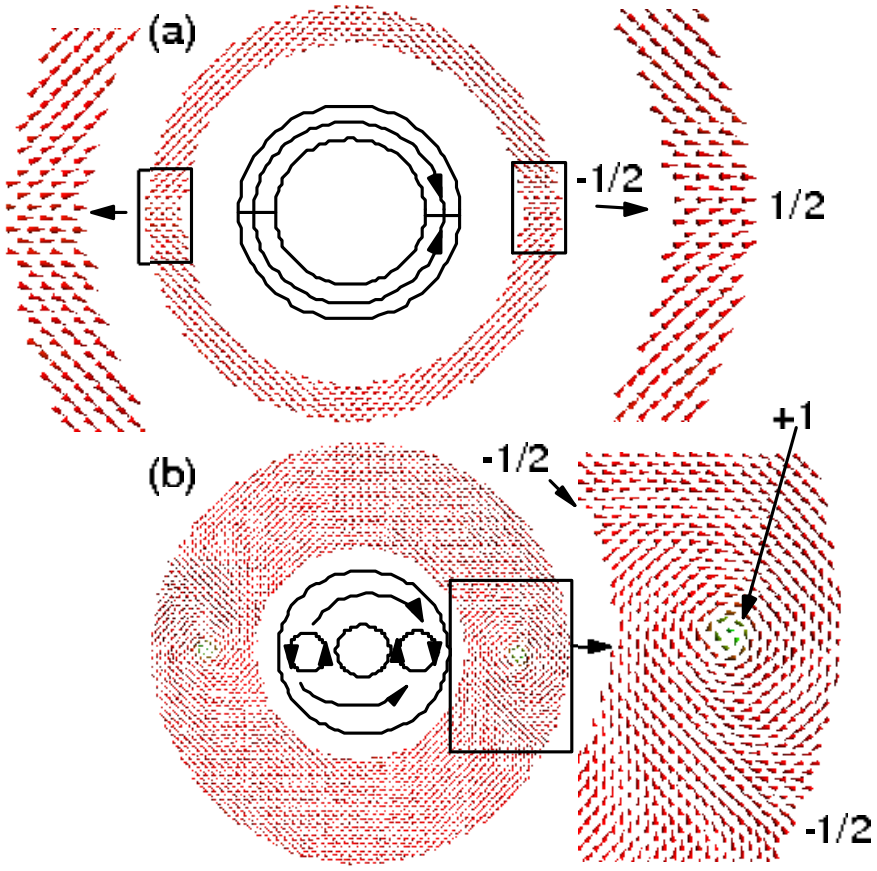

FIG. 4: (color online) Head-to-head domain wall. (a) onion state with transverse domain wall; (b) onion state with vortex domain wall. The numbers in the figure indicate the type of the topological defect.

vortex defect at the center of the rim.[21]

Recently a new category of metastable states has been discovered[33] in relatively small rings made of both Co and permalloy with $R_o \sim 180 - 520nm, w \sim 30 - 200nm, h \sim 10nm$: the twisted states (T) (or saddle state[34]). These states are characterized by 360^o domain walls [35, 36] (see Fig. 6), which have previously been reported in narrow thin film strips. [37, 38] They are shown to be stable within a field range of several hundred Os [33]. Furthermore, they have low stray fields and are easy to control by current, which makes them attractive for data storage applications. There can be more than one 360^o domain wall in rings, resulting in a multi-twisted state. The 360^o domain walls can be viewed as two transverse domain walls (Fig. 6(b)). The attraction between the two transverse walls occurs because they have opposite senses of rotation. This tendency is balanced by the

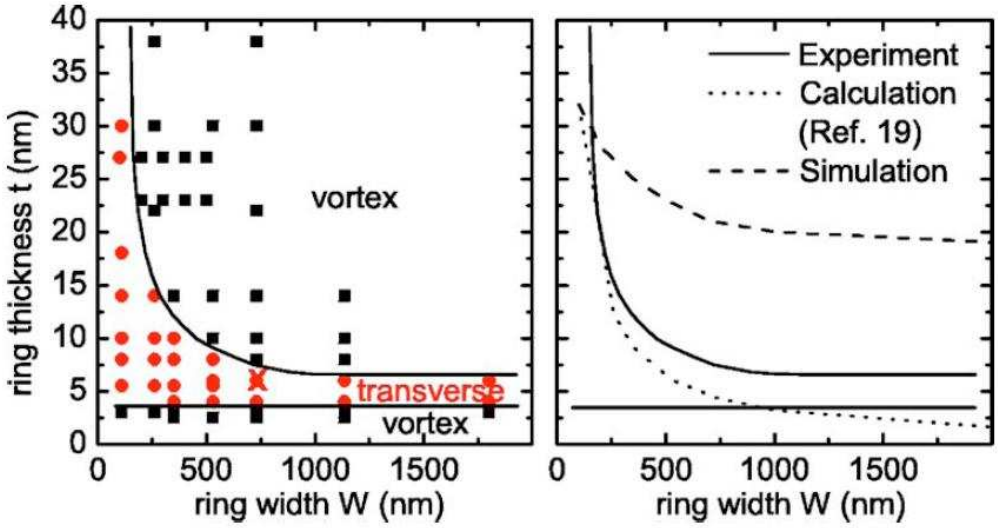

FIG. 5: [32](©Reused with permission from M. Laufenberg, Applied Physics Letters, 88, 052507 (2006). Copyright 2006, American Institute of Physics.) (color online) "(a) Experimental phase diagram for head-to-head domain walls in NiFe rings at room temperature. Black squares indicate vortex walls and red circles transverse walls. The phase boundaries are shown as solid lines. (b) A comparison of the upper experimental phase boundary (solid line) with results from calculations (dotted line) and micromagnetic simulations (dashed line). Close to the phase boundaries, both wall types can be observed in nominally identical samples due to slight geometrical variations. The thermally activated wall transitions shown were observed for the ring geometry marked with a red cross (W=730 nm, t=7 nm)."

exchange energy in the region between the walls. The existence of this domain wall can also be understood fairly easily by topological arguments, referring to the properties (iv) and (vi) of topological defects in Sec. II. When the width is small, the two transverse domain walls have the same defect on the same side, and they are stable. So these edge defects cannot annihilate, resulting in a 360^o domain wall. When the width is larger, however, one of the $\omega = +1/2$ defects becomes unstable and transforms into a $\omega = -1/2$ defect by introducing a vortex into the center of the rim. Then the two transverse domain walls are able to annihilate each other, resulting in a vortex state. Therefore, only a portion of the region of stable transverse wall in the phase diagram Fig. 5 can possibly hold twisted states. Twisted states in large rings have almost zero remanence, so magnetization is incapable of distinguishing between vortex and twisted states and other quantities must be used. Toroidal

moment[39] and winding number are supplementary order parameter candidates.

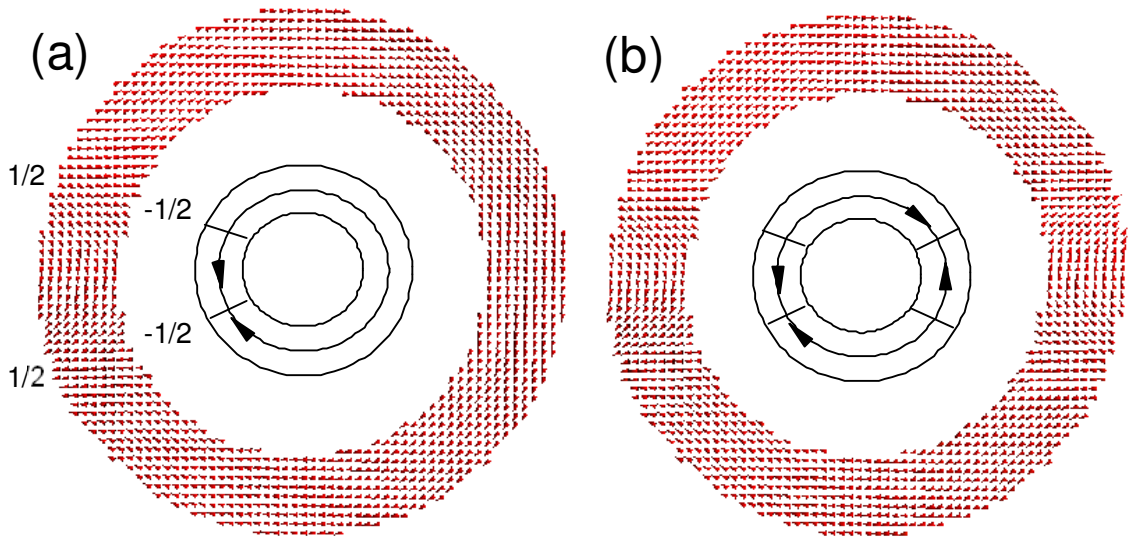

FIG. 6: (color online) Twisted states: (a) with single 360^o domain wall, (b) with two 360^o domain walls. The numbers in the figure indicate the type of defects.

In the presence of an external magnetic field, several other states exist: wave states and shifted vortex core states. They usually exist in very thick rings, which is of less interest for practical reasons. Regarding the effect of crystalline anisotropy, it stabilizes quasi uniform states (like onion states) and imposes some additional domain structures.

IV. SWITCHING PROCESSES

For data storage applications, understanding switching processes is crucial. The main effort is directed towards identifying simple reproducible switching processes and reliable sensitive detection techniques. Meanwhile, in terms of fundamental physics, the understanding of switching processes is just as important. As picosecond and nanometer time and spatial resolution detection techniques are still limited, the microscopic details of switching processes and other dynamic transitions are currently mainly investigated by micromagnetic simulations. One issue that is hard to quantify is the distribution of the switching field. Computationally, the transition in the hysteresis curve is very sharp, while the experimental curves have a broad transition region caused by edge roughness and defects.

The traditional way of studying switching processes is by applying a uniform magnetic

field with changing magnitude. Motivated by the vortex configuration, circular fields are also studied in order to switch the two vortex states with opposite circulation. Here we mainly discuss the uniform field switching case and say a few words about the circular field afterwards.

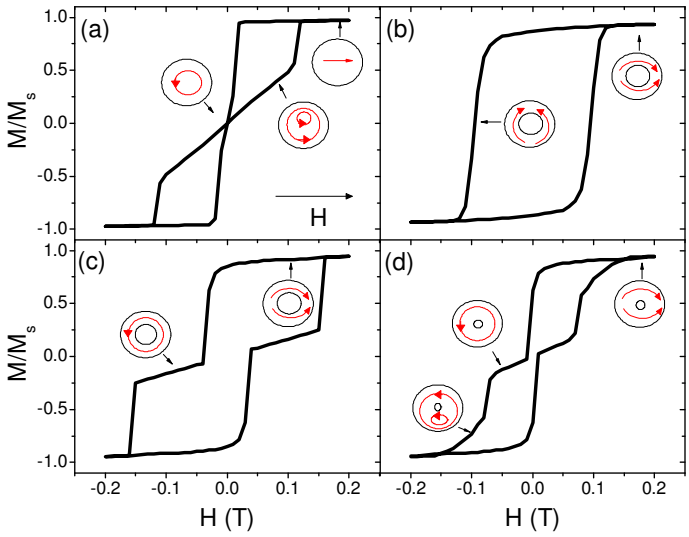

FIG. 7: (color online) Schematic switching process and hysteresis: (a) hysteresis of magnetic discs, (b) one-step switching of rings, (c) double switching of rings, (d) triple switching of rings.

A. Uniform field

With a uniform field, three types of typical hysteresis curves are identified:

1. One-step or single switching

This is a direct onion-to-onion-state switching (O-O). Fig.7(b)) shows a typical hysteresis curve. In this process, an onion state is reversed to the opposite onion state directly. This process is usually only observed experimentally in small rings, especially in the thin film limit (small h). Theoretically speaking, it should happen in much thicker system if the ring is perfectly symmetric, as it is observed in simulations. For real systems, however, there always exists some sort of asymmetry caused either by defects or by the environment. When asymmetry exists, the system tends to fall into its true ground vortex state, which will result

in a double switching process.

It is believed that the switching mechanism is simply a coherent rotation, where two domain walls move in the same rotational direction. This can easily be observed computationally if one intentionally introduces some sort of asymmetry into the system.

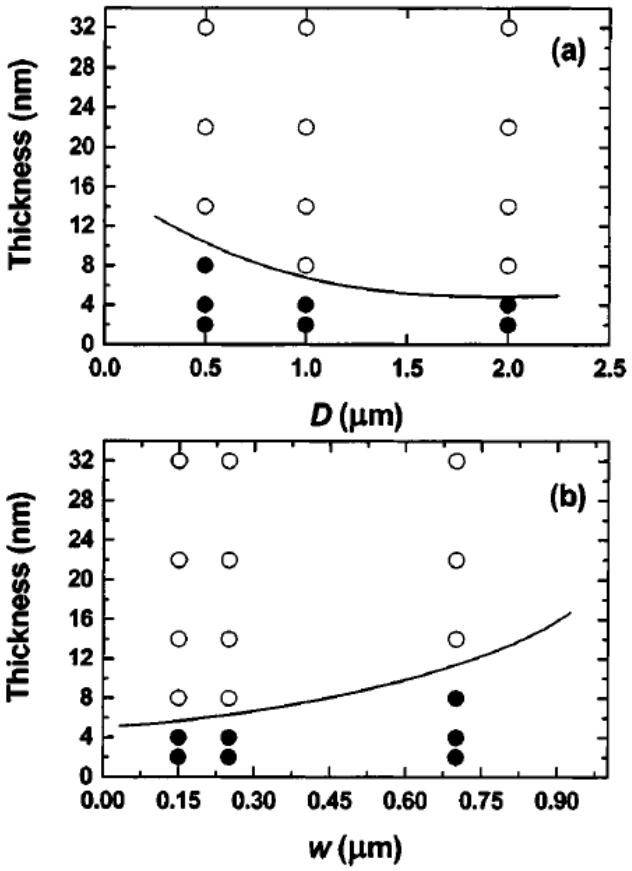

FIG. 8: [40](©Reused with permission from Y. G. Yoo, Applied Physics Letters, 82, 2470 (2003). Copyright 2003, American Institute of Physics.) "Phase diagrams of two-step switching (open circles) and single switching (full circles) as a function the ring geometrical parameters. (a) For a ring width of 0.25 mm. (b) For a ring diameter of 2 mm. The solid lines define the boundary between the two different switching regimes."

Yoo *et al*[40] offered experimental phase diagrams for Co rings with constant width and R_o (equivalent to $D/2$ in Fig. 8) and varying height $2 \sim 34nm$. They conclude that the main geometric factor is the film thickness. When $h < 6nm$, the above one-step switching happens, while otherwise it is two-step switching. For small radii this is not necessarily true, since they only study $R_o > 500nm$. Rings with large radii resemble straight strips very well.

With shrinking radius, however, the story is different. Since magnetic processes including nucleation and annihilation depend strongly on the curvature, small rings can behave quite differently from their bigger counterparts.

2. Two-step or double switching

The dominant switching process for magnetic rings is O-V-O switching or O-T-O switching (see Fig. 7(c)), since the inevitable intrinsic asymmetry stimulates this process. A large regime in the geometric phase diagram falls into this category. In most cases the remanence state starting from saturation is an onion state, and both transitions occur at negative field. When the element is very thick, the remanence state can be a vortex state, i.e. the first transition field is positive.[25, 30] This behavior is found for elements near the boundary between double and triple switching in the switching phase diagrams. The mechanisms of the two steps are discussed separately below.

For O-V or O-T, two possibilities exist, depending on whether it is initiated by domain wall motion or nucleation.

(i) Nucleation and buckling: a strong buckling of the magnetization happens first in one arm of the onion state where the magnetic moments are antiparallel to the external field, followed by a nucleation of a vortex passing through the arm[25, 26]. This process is not typical in two step transitions. Rather, it happens in some shifted inner circle rings or relatively wide rings. The transition field can be positive, resulting in a vortex state at remanence. It is similar to the triple switching-process, so it can also be regarded as a transient process.

(ii) Nucleation free and domain wall motion: one wall is pinned more than the other due to some sort of asymmetry, so that the other wall moves towards it. When the two walls get close to each other, two things could happen: (a) The annihilation process. This is possible only if the ring is sufficiently wide (say larger than $10nm$); (b) 360^o domain walls which are found to exist for narrow and small rings recently[33]. The states formed are twisted states which have been discussed in the previous section. It is interesting and enlightening to understand this process from the topological point of view. As is shown in Sec.III, each of the transverse domain walls consist of two half-vortices: one $\omega = -1/2$ defect on the outer edge and one $\omega = +1/2$ defect on the inner edge. The vortex state cannot form in

arbitrarily thin rings since the half vortices with the same winding number cannot annihilate directly and they cannot move to bulk either. Only when the vortex wall is also an energy minimum, one of the $\omega = +1/2$ edge defects can emit a $\omega = +1$ vortex into the bulk and transform into a $\omega = -1/2$ defect. The emitted vortex will travel to the other side and turn the $\omega = -1/2$ defect into a $\omega = +1/2$ defect.[20, 34] Then the edge defects can annihilate. Overall, the choice of the above processes depends strongly on the ring width, but less so on R_o and h (see Fig. 8). These two processes both happen for relatively small widths.

The V-O transition is sometimes called a first magnetization curve. In the half of the ring with magnetization antiparallel to magnetic field $\vec{H}$, a vortex domain wall nucleates at the inner side of the rim and passes through it perpendicular to $\vec{H}$. In the meantime two transverse head-to-head domain-wall-like structures appear next to the vortex and quickly propagate in opposite directions, forming the final onion state. This process is mainly shape dependent and has little to do with anisotropy, because it depends on how easy it is to form a vortex wall on the edge, which can be assisted by the edge imperfection (or roughness). As expected, this process depends also on the local curvature of the ring. Since the local curvature and edge roughness affect small rings more, the distribution of the switching field will be larger in these systems. However the magnitude of transition field H_c is insensitive to the radius. It increases with height h[41] since thicker elements favor vortex structures, and decreases with width as the vortex state is more stable in thin rings. The nucleation requires a large twisting of the spins, which is harder to achieve in thin rings. Simulations tend to give higher H_c in the absence of defects, but defects are known to reduce H_c. This discrepancy is more severe for thin rings.

The field distribution of O-V is typically larger than in the V-O case and can mainly be attributed to the variation of intrinsic defects among different rings. As temperature tends to wipe out the effects due to defects, i.e. thermal fluctuation make it easier to overcome the local energy barrier induced by defects, the distribution becomes larger when the temperature goes down. This is a little bit surprising at first glance. However, this conclusion can be used to determine whether defects are responsible for the field distribution. If the distribution depends strongly on temperature, then defects are important. Generally speaking, transitions involving nucleation processes are less prone to defects and thermal fluctuation than processes involving domain wall or vortex core motion.[42] Since defects always exist, simulations at 0K for perfect rings mimic more, in some sense, the experimental

situation at high temperature.

3. Triple switching

This process involve three intermediate steps: O-V-VC-O. [25, 42, 43] It is similar to O-V-O except that the vortex state does not deform into an onion state abruptly, but nucleates a vortex core in one arm, and the core then moves slowly to the outer rim. To some extent, it is similar to the switching process of magnetic discs where the core in the vortex state is shifted by a magnetic field and finally exits at the boundary (see Fig. 7(a)). To see this, Steiner *et al* [25] have shown a sequence of hysteresis curves with various inner radii R_i from the disc limit ($R_i = 0$). The field distribution of the V-VC transition is affected little by temperature, so it is affected little by defects. On the other hand the VC-O is process affected strongly by temperature, so defects play an important role here as cores can be pinned by defects. The triple switching process only exists for thick and very wide rings. Since these rings lack the advantages of rings mentioned before, this switching process is less interesting and less studied.

Regarding the effects of anisotropy, it generally suppresses the field distribution and increases the switching field. One curious observation is that ring structures make the hard axis of the cubic anisotropy into the global easy axis[22].

B. Circular field

Circular fields are interesting because they can be naturally generated by a perpendicular current through the disc center. This design is especially suitable for rings, as there is a hole in the center to deposit a nanodot to conduct current. As a result current-induced switching can be achieved, which is essential for data storage applications. At first, a circular field was proposed to switch the vortex state into opposite circulation[4], but it requires a fairly large current density and involves some fairly complicated transient states. Recently, after the twisted states were discovered, a new scheme was proposed.[35, 36] As is shown in Fig. 9, switching is adjusted between two twisted states with the 360^o domain wall located in the left and right rim (or any two positions along a diameter). This switching requires low current and has a very clean transition process which only involves a domain wall movement.

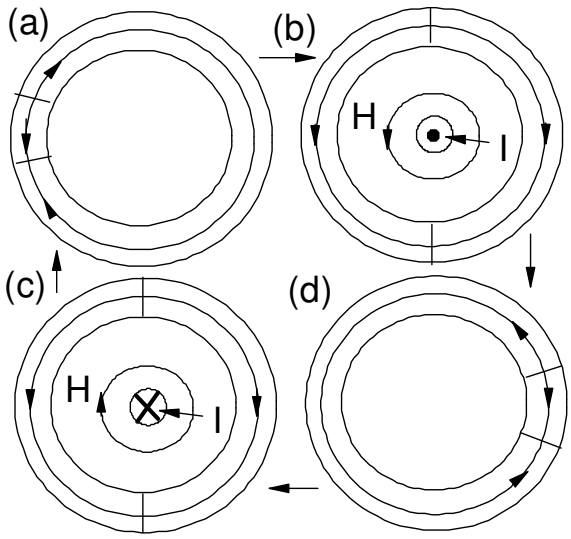

FIG. 9: Schematic diagram of twisted state reversal by circular field.

In addition, it is very fast.

V. APPLICATIONS

Nanomagnets are featured in many applications. One of the most important is in data storage devices. Three schemes have been proposed[44] for nanorings: (i) two onion states, similar to the traditional oblong memory element, except that the switching current is significantly less. However, the stray field is an obstacle for high density storage; (ii) two vortex states with different circulation, studied most intensively but requiring a relatively high current density [4]; (iii) two twisted states, most promising because of the low stray field and low current. [36]

For the first choice, Kläui *et al* [22] have performed a dynamics switching study. They used magnetic pulses to switch the magnetization. They found that switching is only possible when $H * \Delta t \approx 5 * 10^{-12} T * s$, keeping $H > 20mT$ and $\Delta t > 50ps$. The switching time is T=0.4ns, so that the possible switching rate is about 1.25GHz ($= 1/(2T)$).

Most attention has been focused on the second choice, for this one utilizes all the benefits of nanorings. Manmade asymmetry offers a way to control the vortex circulation. Several techniques are available: shifted inner circle[45, 46], notches[40], and elongated shapes like ellipses[47, 48]. Some works[45, 49] claim that even when there exists asymmetry, the

switching process is still a stochastic process due to the thermal fluctuation. Some rings in an array may follow O-O switching while other rings may follow O-V-O. Even for the same ring the circulation may not be deterministic, so the strength of the asymmetry needed is still an important open question.

Recently, increasing attention has been given to the third possibility[35, 36, 44], as it is suggested that the twisted state can be switched very easily by a small circular current and can achieve high speed. Experimental evidence is needed to confirm the idea.

Another obstacle to application is that ring arrays always show a wide distribution of switching fields. To make the application realistic, the width of the distribution has to be reduced. The distribution is attributed to both the interior and exterior defects. Though the influence is qualitatively known, quantitative analysis is still missing. Even though one would like to get rid of defects as much as possible in most cases, they can also be used to engineer the switching behavior. [47, 50].

VI. CONCLUSIONS

We have reviewed current results in the study of ferromagnetic rings, with emphasis on switching processes. Ring structures feature many advantages including being stable and insensitive to edge imperfection and completely stray field free. Ring arrays give an ultimate area storage density of about $0.25 Tbits/cm^2$. We covered all possible states identified numerically and experimentally until now, among which vortex, onion and twisted states are discussed in detail, since they are suggested to be candidates for data storage. There are three types of switching processes under uniform field, depending on the geometric parameters of the ring. The double switching, in particular, enjoys tremendous popularity. By introducing engineered asymmetry, the circulation direction of the vortex state can be easily controlled by a uniform field. The mechanisms of these switching processes were explained carefully in detail and topological argument were shown to be enlightening. On the other hand, circular field switching is easy to generate, and is suitable to switch the twisted state. Finally applications and limitations were briefly discussed.

Acknowledgement: We would like to thank Noah Jacobson and Yaqi Tao for useful discussions. Computing facilities were generously provided by the University of Southern

California high-performance supercomputing center. We also acknowledge financial support by the Department of Energy under grant DE-FG02-05ER46240.

[1] K. De'Bell, A. B. Maclsaac, and J. P. Whitehead, Rev. Mod. Phys. **72(1)**, 225 (2000).

[2] J. I. Martin, J. Nogues, J. L. V. K. liu, and I. K. Schuller, J. Magn. Magn. Mater. **256**, 449 (2003).

[3] R. P. Cowburn, J. Phys. D: Appl. Phys. **33**, R1 (2001).

[4] J. G. Zhu, Y. Zheng, and G. A. Prinz, J. Appl. Phys. (2000).

[5] J. Akerman, Science **308**, 508 (2005).

[6] G. A. Prinz, Science **282**, 1660 (1998).

[7] M. M. Miller, G. A. Prinz, S. F. Cheng, and S. Bounnak, Appl. Phys. Lett. **81**, 2211 (2002).

[8] M. Kl*äui*, J. Phys.: Condens. Matter **20**, 313001 (2008).

[9] J. Filer and T. Schrefl, J. Phys. D: Appl. Phys. **33**, R135 (2000).

[10] E. M. Lifshiftz and L. P. Pitaevskii, *Statistical Physics, part 2* (Reed Educational and Professional Publishing Ltd., 1980), pp. 286–288.

[11] Gilbert, Phys. Rev. **100**, 1243 (1955).

[12] L. Greengard and V. Rokhlin, J. Comp. Phys. **73**, 325 (1987).

[13] W. Zhang and S. Haas, *arxiv:0810.0233* (2008).

[14] M. J. Donahue and D. G. Porter, *Oommf user's guide (nist, gaithersburg, md)* (1999).

[15] W. Scholz, *http://magnet.atp.tuwien.ac.at/scholz/magpar/* (2003).

[16] H. Fangohr, T. Fischbacher, M. Franchin, and et al, *http://nmag.soton.ac.uk/* (2007).

[17] G. Brown, T. C. Schulthess, D. M. Apalkov, and P. B. Visscher, IEEE Trans. Magn. **40**, 2146 (2004).

[18] C. Kittel, *Introduction to Solid State Physics, vii ed.* (John Wiley and Sons, 1996), pp. 565–566.

[19] N. D. Mermin, Rev. Mod. Phys. **51**, 591 (1979).

[20] O. Tchernyshyov and G. W. Chern, Phys. Rev. Lett. **95**, 197204 (2005).

[21] H. Youk, G. W. Chern, K. Merit, B. Oppenheimer, and O. Tchernyshyov, J. Appl. Phys. **99**, 08B101 (2005).

[22] M. Kläui, C. A. F. Vaz, L. Lopez-Diaz, and J. A. C. Bland, J. Phys.: Condens. Matter **15**, R985 (2003).

[23] D. Wortmann, S. Heinze, and P. K. *et al*, Phys. Rev. Lett. **86**, 4132 (2001).

[24] C. L. Gao, W. Wulfhekel, and J. Kirschner, Phys. Rev. Lett. **101**, 267205 (2008).

[25] M. Steiner and J. Nitta, Appl. Phys. Lett. **84**, 939 (2004).

[26] F. Giesen, J. Podbielski, B. Botters, and D. Grundler, Phys. Rev. B **75**, 184428 (2007).

[27] M. Beleggia, J. W. Lau, M. A. Schofield, Y. Zhu, S. Tandon, and M. DeGraef, J. Magn. Magn. Mater. **301**, 131 (2006).

[28] P. Landeros, J. Escrig, D. Altbir, M. Bahiana, and J. d'Albuquerque e Castro, J. Appl. Phys. **100**, 044311 (2006).

[29] W. Zhang, R. Singh, N. Bray-Ali, and S. Haas, Phys. Rev. B **77**, 144428 (2008).

[30] S. P. Li, D. Peyrade, M. Natali, A. Lebib, Y. Chen, U. Ebels, L. D. Buda, and K. Ounadjela, Phys. Rev. Lett. **86**, 1102 (2001).

[31] R. D.McMichael and M. J. Donahue, IEEE Trans. Magn. **33**, 4167 (1997).

[32] M. Laufenberg, D. Backes, W. Buhrer, D. Bedau, M. Kläui, and et al, Appl. Phys. Lett. **88**, 052507 (2006).

[33] F. J. Castano, C. A. Ross, C. Frandsen, A. Eilez, D. gil, H. I. . Smith, M. Redjdal, and F. B. Humphrey, Phys. Rev. B **67**, 184425 (2003).

[34] G. D. Chaves-O'Flynn, A. D. Kent, and D. L. Stein, *arxiv:0811.4440v1* (2008).

[35] C. B. Muratov and V. V. Osipov, J. Appl. Phys. **104**, 053908 (2008).

[36] C. B. Muratov and V. V. Osipov, *arxiv:0811.4663v1* (2008).

[37] Y. Zheng and J. G. Zhu, IEEE Trans. Magn. **33**, 3286 (1997).

[38] X. Portier and A. Petford-Long, Appl. Phys. Lett. (2000).

[39] S. Prosandeev and L. Bellaiche, Phys. Rev. B **77**, 060101(R) (2008).

[40] Y. G. Yoo, M. Kläui, C. A. F. Vaz, L. J. Heyderman, and J. A. C. Bland, Appl. Phys. Lett. **82**, 2470 (2003).

[41] M. Kläui, L. Lopez-Diaz, J. Rothman, C. A. F. Vaz, J. A. C. Bland, and Z. Cui, J. Magn. Magn. Mater. **240**, 7 (2002).

[42] M. Kläui and et al, Appl. Phys. Lett. **84**, 951 (2004).

[43] M. Steiner, G. Meier, U. Merkt, and J. Nitta, Physica E (2004).

[44] C. L. Chien, F. Q. Zhu, and J. G. Zhu, Phys. Today (2007).

[45] F. Q. Zhu, G. W. Chern, O. Tchernyshyov, X. C. Zhu, J. G. Zhu, and C. L. Chien, Phys. Rev. Lett. (2006).

[46] S. Prosandeev, I. Ponomareva, I. Kornev, and L. Bellaiche, Phys. Rev. Lett. **100**, 047201 (2008).

[47] N. Agarwal, D. J. Smith, and M. R. McCartney, J. Appl. Phys. **102**, 023911 (2007).

[48] N. Singh, S. Goolaup, W. Tan, A. O. Adeyeye, and N. Balasubramaniam, Phys. Rev. B **75**, 104407 (2007).

[49] T. J. Hayward, T. A. Moore, D. H. Y. Tse, J. A. C. Bland, F. J. Castano, and C. A. Ross, Phys. Rev. B **72**, 184430 (2005).

[50] X. S. Gao, A. O. Adeyeye, and C. A. Ross, J. Appl. Phys. **103**, 063906 (2008).